Acta of Bioengineering and Biomechanics
Vol. 16, No. 4, 2014

Original paper
DOI: 10.5277/ABB-00010-2014-02

Ion Move Brownian Dynamics (IMBD) – Simulations of Ion Transport

MONIKA KURCZYNSKA*, MALGORZATA KOTULSKA

Department of Biomedical Engineering, Wroclaw University of Technology, Wroclaw, Poland.

Purpose: Comparison of the computed characteristics and physiological measurement of ion transport through transmembrane proteins could be a useful method to assess the quality of protein structures. Simulations of ion transport should be detailed but also time-efficient.

Methods: The most accurate method could be Molecular Dynamics (MD), which is very time-consuming, hence is not used for this purpose. The model which includes ion-ion interactions and reduces the simulation time by excluding water, protein and lipid molecules is Brownian Dynamics (BD). In this paper a new computer program for BD simulation of the ion transport is presented. We evaluate two methods for calculating the pore accessibility (round and irregular shape) and two representations of ion sizes (van der Waals diameter and one voxel).

Results: Ion Move Brownian Dynamics (IMBD) was tested with two nanopores: alpha-hemolysin and potassium channel KcsA. In both cases during the simulation an ion passed through the pore in less than 32 ns. Although two types of ions were in solution (potassium and chloride), only ions which agreed with the selectivity properties of the channels passed through the pores.

Conclusions: IMBD is a new tool for the ion transport modelling, which can be used in the simulations of wide and narrow pores.

Key words: *alpha-hemolysin, Brownian dynamics, ion transport, potassium channel, model quality assessment*

1. Introduction

The transport of ions and small molecules through the membrane is a fundamental phenomenon of cells, and is enabled by many types of transmembrane proteins. To discover the molecular functions of these proteins, their structures are needed. X-ray crystallography of transmembrane proteins is difficult to obtain because these proteins are relatively large and their natural environment is lipid membrane. Currently, only 2,099 transmembrane protein structures are known (PDBTM, as of April 2014) [1], which is only 2% of all deposited protein structures (PDB, as of April 2014) [2], while transmembrane proteins correspond with 25% of genes [3]. Scientists have been working on methods to predict transmembrane proteins with a variety of computational methods [4], [5]. The studies of ion channel structures broaden our knowledge about their pathological behaviours, which can lead to diseases [6], [7].

Apart from the modelling methods, the quality assessment of the structural models is an important step during this process. The most common methods for assessing the models are based on the comparison of the structural properties of a model and the features observed in high-resolution protein structures [8], [9]. For example, the program Gaia [8] calculates the number of steric clashes, the accessible surface area, bond lengths, angles, dihedrals and rotamers. The last competition for modelling protein structure, Critical Assessment of Protein Structure Prediction (CASP10), collected 37 methods in the model quality assessment (MQP) category [9], of which the best 12 methods were statistically indistinguishable. The new approach in MQP is the analysis of similarity between the func-

* Corresponding author: Monika Kurczynska, Department of Biomedical Engineering, Wroclaw University of Technology, Wybrzeze Wyspianskiego 27, 50-370 Wroclaw, Poland. Tel: +48 71 320 44 61, e-mail: monika.kurczynska@pwr.edu.pl

Received: April 16th, 2014
Accepted for publication: April 21st, 2014

tional features of the model and proteins in the databases [10], or the comparison of the computed functional characteristics of the model and physiological measurement of the protein [11].

To obtain the voltage-current curve of an ion channel model, three basic methods, reviewed in Kuyucak et al. [12], can be used: Molecular Dynamics (MD), Brownian Dynamics (BD) and the electrodiffusion Poisson–Nerst–Planck model (PNP). MD is based on classical Newtonian physics. The trajectories of all the atoms in the simulation system, including protein and water molecules, are calculated at each time step. This approach requires a great deal of computational power, even using supercomputers. On the other hand, MD simulations are very detailed at the atomic level, so experimental observations may be explained using the results of the simulations. However, MD is too time-consuming as a method to assess the quality of structural model collections, and has never been used for this purpose. Hence, less accurate, but more time-efficient approaches, are considered. One of them is the PNP model, which does not require vast computing resources for a large number of atoms over a long time scale, because the whole simulation system is represented by a continuum medium. The studies by Noskov et al. [13], Cozmuta et al. [14] and Dyrka et al. [15] have shown the potential of the PNP model in protein structure analysis. A more detailed way of ion transport modelling is the BD model, which is built from a continuum solvent and the discrete representation of ions, whose trajectories are recorded. There are a number of ion transport studies using BD, e.g. [16]–[19], but they are either not freely available or generally tested with wide pores. They include GCMC/BD [19], SDA [22], UHBD [23], and BD_BOX [24]. One program which has ony been tested with wide pores is GCMC/BD [19]. Lee et al. [19] tested their program with beta-barrel pores: OmpF with a radius of 13 Å, VDAC with a radius of 15 Å, and α-hemolysin with a radius of 14 Å. Similarly, Krammer et al. [20] used GCMC/BD with VDAC. Biase et al. [21] used GCMC/BD with a cylindrical pore, whose radius was 9 Å, and for α-hemolysin. We tried to use GCMC/BD with potassium channel KcsA, which has a narrow pore of radius 1.5 Å, but the program generated mistakes during the pore formation process. According to the SDA [22] website, SDA simulates the diffusional association of two molecules or a molecule to a solid state surface. We did not find a protocol for ion transport simulation with SDA. Most of the papers in which SDA was used to describe the interaction process between two molecules. Similar to SDA, UHBD [23] is also devoted to simulating two molecules and the internal dynamics of a protein. There is no simple way of modelling an ion channel flow with UHBD. BD_BOX [24] offers BD calculations using advanced computer techniques, which improve computing efficiency, and it can be used to simulate interactions between molecules.

Our main goal is to use the BD algorithm to obtain the current-voltage curve for structural models of transmembrane proteins, including wide bacterial pores and narrow ionic channels. The BD simulation results will be used to assess the quality of structural channel models. We need a BD program suitable for modelling ion transport through narrow pores and which would also be user friendly.

In this study, we present the first version of the Ion Move Brownian Dynamics (IMBD) – a program for running simulations of ion transport through nanopores. Our application can be used also for modelling flow in channels with narrow pores. We present tests of IMBD with two different biological nanopores, representing different dimensional characteristics.

2. Materials and methods

Theoretical background of IMBD

IMBD is based on Brownian Dynamics (BD), which treats ion movement in water solutions as a Brownian motion. Using BD we can follow the trajectory of ions, reducing the simulation time by excluding explicit representation of atoms of a protein, a lipid bilayer and water molecules. The protein and the lipid membrane are defined in the simulation by exclusion and potential grids. Water molecules are incorporated into the model by random and friction forces acting on the ions. Subsequent positions of each ion are calculated by Langevin's stochastic equation [25]

$$m_i \frac{dv_i}{dt} = - m_i \gamma_i v_i + R_i + Fs_i \tag{1}$$

where m_i is the mass of the i-th ion, v_i is the velocity of the i-th ion, γ_i is the friction coefficient of the i-th ion, R_i is the random force, and Fs_i represents the systematic force. The hindrance of water is expressed by the diffusion coefficient, which is linked to the friction coefficient by Einstein's equation [25]

$$\gamma_i = \frac{kT}{m_i D_i} \tag{2}$$

where k is the Boltzman constant, T is the temperature, D_i represents the diffusion coefficient. The value of the random force is obtained from a Gaussian distribution with mean 0 and the variance dependent on the diffusion characteristic of the ion type. The systematic force is represented by the electrostatic interactions: ion-ion, ion-protein and ion-membrane.

The ion and pore dimensions in the simulation system can be defined in various ways. In this study, we evaluate two methods for calculating the pore accessibility and two representations of ion sizes. Four combinations of the algorithm were tested. The first method (*irregular*) for determining pore area chooses every voxel which does not belong to the protein or membrane and is restricted vertically and horizontally with voxels of a protein or membrane. A second idea (*circular*) for calculating the pore accessibility is based on pore symmetry. We compute the biggest circle in each voxel plane normal to the pore axis and we choose the voxels which are inside the circle. The problem of ion representation is related to the cubic representation of the pore, for which we propose two solutions. The *sphere* ion representation uses a sphere with a radius equal to the ion's van der Waals radius and converts it into an angular representation. The *sphere* method sets the voxel as the place where the ion lies if the ion occupies more than half of the voxel. The *point* representation treats the ion as a single voxel which contains the centre of the ion. The ion's size in both cases affects the value of the diffusion coefficient.

Pipeline

The IMBD program consists of 12 modules (Fig. 1) and requires, as input, exclusion and potential grids generated with external software, which are also depicted in Fig. 1. Before running the simulation with IMBD, a PDB structure file should be downloaded from a database. We advise finding the PDB file in the Orientations of Proteins in Membrane database (OPM, http://opm.phar.umich.edu/server.php) [26], because the protein is perpendicularly-oriented and the user does not then need to look for the pore axis. In this case the user should delete the HETATM atoms from the PDB file. The next step is converting the PDB file to the PQR format, which collects extra information about van der Waals radii and the partial charges of all atoms from the PDB file, using PDB2PQR software (www.poissonboltzman.org/pdb2pqr) [27]. Next, the user should run the APBS (http://www.poissonboltzmann.org/apbs/) [28] to obtain the exclusion, charge and potential grids. The potential grids can be used in IMBD but we propose applying potential grids from the 3D PNP Solver (http://www.kotulska-lab.pwr.wroc.pl/ [Download]) [15], because they are better fitted to our algorithm. In opposition to the APBS grids, the potential grids from the 3D PNP Solver provide the potential which includes the transmembrane potential gradient and ions in the pore.

The first step in using the IMBD program (Fig. 1-1; Input parameters) is defining the input parameters, which contain information about the ions (charge, radius, mass, concentration, diffusion coefficient and velocity in bulk), the membrane (thickness, position relative to the protein), the dielectric constant of all mediums, the file names of the exclusion and potential grids, the transmembrane potential, temperature, time step, simulation time and save step. The program also uses optional parameters to narrow the simulation area, which reduces the CPU-time of the simulation, and improves the quality of the membrane building

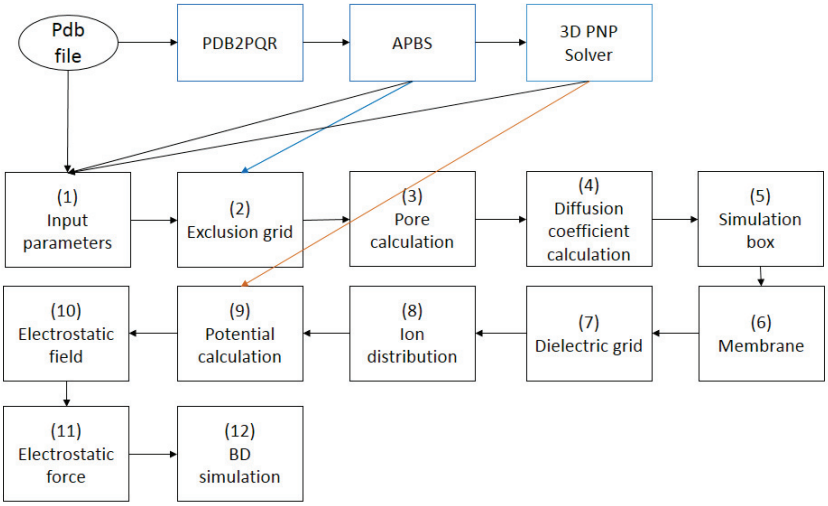

Fig. 1. The pipeline of IMBD

process. These parameters can be added at the beginning but also can be modified after the reading and visualisation of the exclusion grids. The building of the discrete protein model (Fig. 1-2; Exclusion grid) is based on the exclusion maps from the APBS. Step 3 (Fig. 1-3; Pore calculation) calculates the pore accessibility using two different methods: *irregular* and *circular* (see 2.1). Step 4 (Fig. 1-4; Diffusion coefficient calculation) generates a diffusion coefficient grid based on the pore area and the hydrodynamic model (HD) [29]:

$$D\left(\frac{R_{\text{ion}}}{R_{\text{pore}}}\right)=\frac{D_0}{A+B\cdot\exp\left(\frac{R_{\text{ion}}}{C\cdot R_{\text{pore}}}\right)+E\cdot\exp\left(\frac{R_{\text{ion}}}{F\cdot R_{\text{pore}}}\right)} \tag{3}$$

where D_0, R_{ion}, R_{pore} are the diffusion constant of the ion in the bulk and the radius of the ion and the pore. A, B, C, E, F are the coefficients of the function. The values for the best approximations for α-hemolysin are [29]: A = 0.64309, B = 0.0044, C = 0.06894, E = 0.35647, F = 0.198409. To reduce the calculation time during the simulation the diffusion coefficient grid is converted to the friction coefficient grid. Step 5 (Fig. 1-5; Simulation box) sets the simulation box using optional parameters. Usually this module lets the user reduce the simulation area only to the pore and buffer region. In the next step (Fig. 1-6; Membrane) the membrane is built as an inaccessible region for ions. The membrane is defined as voxels which do not belong to the protein, are not part of the pore and are located between coordinates chosen by the user. When the whole system is defined, the program sets (Fig. 1-7; Dielectric grid) the dielectric constant for each voxel according to the type of voxel occupancy (protein, membrane, pore, bulk), based on the values of the input parameters (Fig. 1-1). The next step (Fig. 1-8; Ion distribution) generates the initial ion distribution in the simulation box based on the voxels which do not belong to the protein or membrane. Before the simulation runs, the potential grids are read (Fig. 1-9; Potential calculation) and all electrostatic properties of the system are set (Fig. 1-10; Electrostatic field). Calculating the electrostatic force before the simulation permits us to save CPU-time (Fig. 1-11; Electrostatic forces). The last step (Fig. 1-12; BD simulation) runs the Brownian Dynamics simulation of the whole system.

In each step of the simulation, IMBD computes the Coulomb interaction between the ion and the other ions, which are closer than the cut-off values, random forces acting on the ion and the new position of the ion. The new ion position is verified in 3 steps. Firstly, the program checks if the ion is out of the system. The second step analyses whether the ion collides with the protein or membrane. If the ion's next move leads to an occupied site within the protein or membrane voxel, an elastic collision happens, which means the ion has the same position as before but the velocity acts in the opposite direction. Step 3 prevents ion-ion collisions. If a collision happens, the ion does not move in this time step. After calculating the new position of all ions in one time step the boundary conditions are ascertained. The ion concentration on both sides of the membrane (the middle of the membrane is set as a border between two regions) is constant and keeps its initial values. If, on one side, the number of ions is higher than the initial conditions, the surplus of ions is reduced. In the opposite situation new ions are added. In our test simulations we set different borders between the two regions. If we used normal boundary conditions we would not see the ion transition through the whole pore, because it would be removed after passing into the middle of the membrane.

Design of the experiment

To test the IMBD program, we selected two nanopores: one wide beta-barrel – alpha-hemolysin (PDB: 7ahl [30]) and one narrow alpha helix ionic channel – potassium channel KcsA (PDB: 3fb8 [31]). The protein structures were downloaded from the OPM database [26].

Alpha-hemolysin is a bacterial protein from *Staphylococcus aureus,* whose monomer forms aggregate into a heptameric channel [29]. Extra wide pores in the cell wall lead to cellular lysis and human disease. Alpha-hemolysin is known to be mildly anion-selective and shows a rectification effect. Its structure (7ahl in PDB) was obtained at a resolution of 1.89 Å with X-ray diffraction and shows that the diameter of the pore is about 14 Å.

Potassium channel KcsA is a bacterial protein from *Escherichia coli*, which was the first ionic channel structure discovered [31]. There are a few structures of different KcsA conformations available in the databases. In our study we used the open-conductive structure PDB: 3fb8, which was obtained at a 3.4 Å resolution via X-ray diffraction. The narrowest pore diameter is about 3 Å and creates the selectivity filter, while the widest part of the channel is about 27 Å. The filter causes more efficient transport of the potassium ions and does not allow other types of ions to pass through the channel.

3. Results

We ran four simulations of each nanopore with four versions of IMBD. The conditions for both systems in each simulation were the same (Table 1), except the simulation time, which was longer for the potassium channel. Only one pair of ions, which had opposing charges, was used in the simulations, because our goal at this stage of the software development was to assess if the algorithm of IMBD works correctly on a single ion.

Table 1. The simulation conditions

		7ahl	3fb8
Dielectric constant	Protein	2	2
	Membrane	2	2
	Pore	40	40
	Solvent	80	80
Temperature [K]		298.15	298.15
Transmembrane potential [mV]		–100	100
Ions	Types	Potassium, chloride	Potassium, chloride
	Charge [*e*]	+1, –1	+1, –1
	Mass [kg]	$6.5\cdot10^{-26}$, $5.9\cdot10^{-26}$	$6.5\cdot10^{-26}$, $5.9\cdot10^{-26}$
	Radius [Å]	1.33, 1.81	1.33, 1.81
	Diffusion coefficient in bulk [m^2/s]	$1.96\cdot10^{-9}$, $2.03\cdot10^{-9}$	$1.96\cdot10^{-9}$, $2.03\cdot10^{-9}$
	Velocity in bulk [m/s]	435, 473	435, 473
	Concentration outside and inside [M]	0, 0.02	0, 0.05
Time step [fs]		10	10
Simulation time [ns]		35	250
Membrane thickness [Å]		23	39
Cutoff for Coulomb forces [Å]		6	6

Figure 2 shows the trajectory projections on a cross-section of the proteins. The starting positions (red points) and final positions (magenta points) for both nanopores are on the other side of the membrane. In both cases single ion transition is shown. Alpha-hemolysin is a wide pore so the ion has more space to move than in the narrow potassium channel. We observed a high density of ion movement in the narrowest part of the pore, because the ion had fewer paths allowing passing to the other side of the membrane.

Figure 3 summarizes the trajectories of ions in alpha-hemolysin simulations obtained with different versions of IMBD. The blue lines indicate the boundary between the inside and outside of the cell, so they indicate whether the ion went through the pore. The simulation time of alpha-hemolysin was 35 ns, because the typical time for a single ion transition in biological channels is 32 ns. We expected that 35 ns is enough to see how the ion moves through the pore. For variants *irregular-sphere* and *circular-sphere* (Fig. 3a and c), which define the ions as a sphere, the simulation time was sufficient for the ion to pass through the pore. In the case of *irregular-sphere* variant the transition time was 33 ns, while in the *circular-sphere* simulation the ion needed only 18 ns. Versions *irregular-sphere* and *circular-sphere* have different algorithms for calculating the pore accessibility. In the case of *circular-sphere*, the shape of the pore is smoother, so the ion does not have as many possibilities as in the *irregular-sphere* to get lodged in the irregular shape of the pore. Moreover, the random force in the simulations causes the differences between the same simulation systems, because its variance is dependent on the diffusion coefficient. In both simulations the chloride anion went through the protein while the potassium ion had problems going

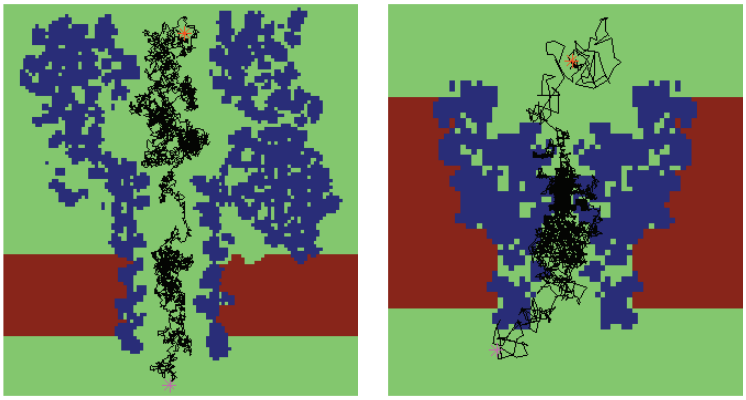

a) b)

Fig. 2. The trajectories of the ions: (a) chloride anion in the 7ahl simulation with irregular-sphere variant, (b) potassium cation in the 3fb8 simulation with irregular-point variant, where blue shows a protein, brown a membrane, black a trajectory, red * a starting position and magenta * a final position

deeper into the pore. This result agrees with the mildly anion-selective property of alpha-hemolysin. In situations when the ion is defined as a single voxel (Fig. 3b and d) we did not observe successful ion transitions. When the ion requires only one free voxel to occupy a new position, the irregular shape of the pore can create a trap where ions may fluctuate before an appropriate path to continue their movement will be found.

In Fig. 3a and c we can observe that the new cations, which appeared after the ion transition through the pore, were added close to the anions. It induced an increase in the electrostatic forces between the two ions (Fig. 4a and c). The charges of the ions have different polarities, so the Coulomb forces stabilize the ions in one position. These configurations of two ions were observed in the last 5 ns of the simulations. In the *irregular-sphere* simulation the ions were much closer to each other than in the *circular-sphere* simulation, because the values of Coulomb forces were ten times higher: 63 nN and 6 nN, respectively. In the

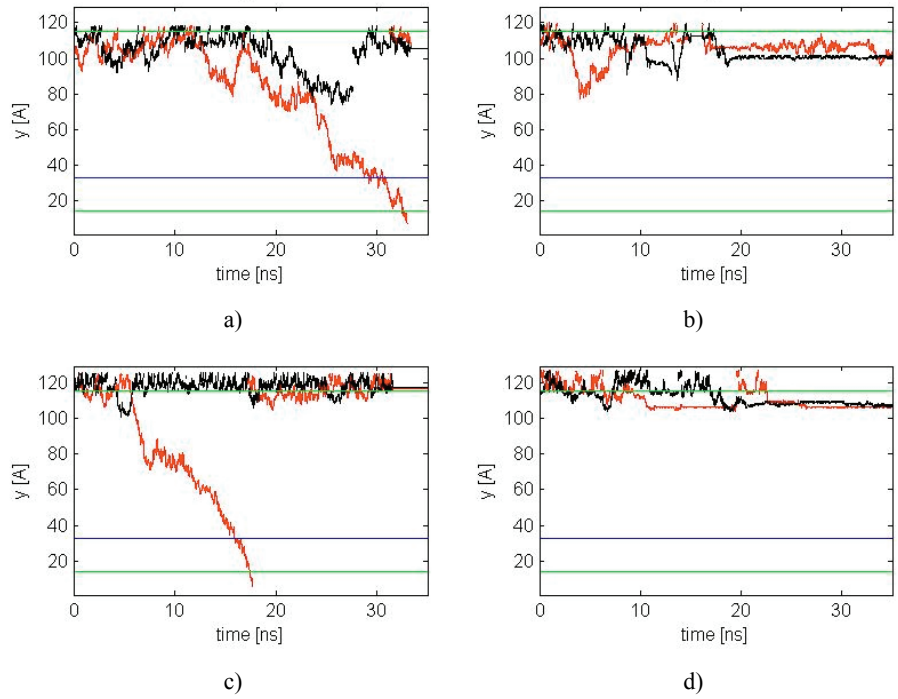

Fig. 3. The trajectories of the ions in 7ahl simulations with: (a) irregular-sphere, (b) irregular-point, (c) circular-sphere, (d) circular-point, where red are the chloride anions, black are the potassium cations, green are the edges of the protein, blue is the middle of the membrane

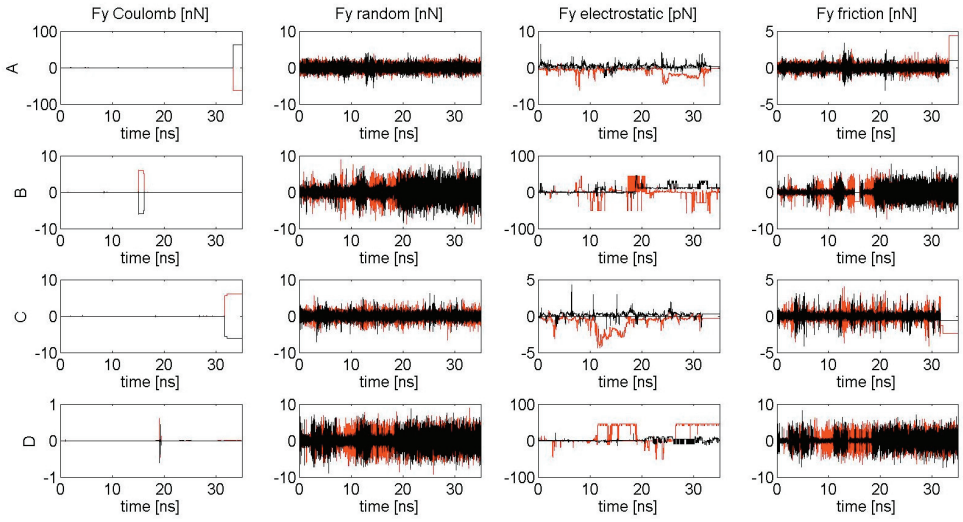

Fig. 4. The forces acting on the ions in 7ahl simulations with: (a) irregular-sphere, (b) irregular-point, (c) circular-sphere, (d) circular-point, where red are the forces acting on the chloride anions, black are the forces acting on the potassium cations

simulation with *irregular-point* (Fig. 4b) we observed the Coulomb force growing to 6 nN in 15 ns and we indicated the ions stopping in one position for 1 ns (Fig. 3b). The last figure presenting Coulomb forces (Fig. 4d) shows the low value of electrostatic interaction at 19 ns, where the value of the force was 0.6 nN.

The random and friction forces should be in the range of nN [25] and in our simulations with each version of IMBD we observed randomly fluctuating values of these forces in the range from 0 to 10 nN (Fig. 4). At the transmembrane potential of 0.1 V the electrostatic forces in the pore, which do not include the Coulomb interactions between ions, should be in the range of pN [25]. In the cases of *irregular-sphere* and *irregular-point* we observed values of the electrostatic forces of less than 10 pN. The relation between these forces and time was not random. The electrostatic forces depended on the position of the ion. The reason for the higher values of the electrostatic forces in Figs. 4 b and d is the representation of the ions. When the ion was represented as a single voxel, so it can be closer to the wall than the spherical ion, we could observe higher single values of the electrostatic potential, which resulted from the higher potential near the protein wall.

Difficulties in the ion's transition through the pore can be solved with the number of ions in the whole simulation. At the beginning, one pair of ions is in the simulation box. If one of them is destroyed a new one is added. If one type of ions has problems moving into the other side of the membrane, it will often be replaced with another ion of randomly attributed initial condition. In the simulation of alpha-hemolysin we observed a larger number of potassium ions than chloride anions (Table 2). The opposite situation is found in the simulation with *circular-point*. However, in this case both types of ions may get lodged in the irregular shape of the pore.

Table 2. The number of the ions in the simulations of 7ahl

	Potassium cations	Chloride anions
irregular-sphere	53	47
irregular-point	21	14
circular-sphere	117	49
circular-point	25	38

Figure 5 shows how the ions move in the potassium channel simulation with four versions of IMBD. Algorithms which define the ion as a sphere (Fig. 5a and c) had problems pushing the ions into the channel. In both simulations the ions were stopped before the entrance of the selectivity filter (y = 81 Å). Finally, the ions in the small area of the pore were close to each other and, as a result, they attracted each other by electrostatic forces. Until the end of the simulation they stuck together in one position.

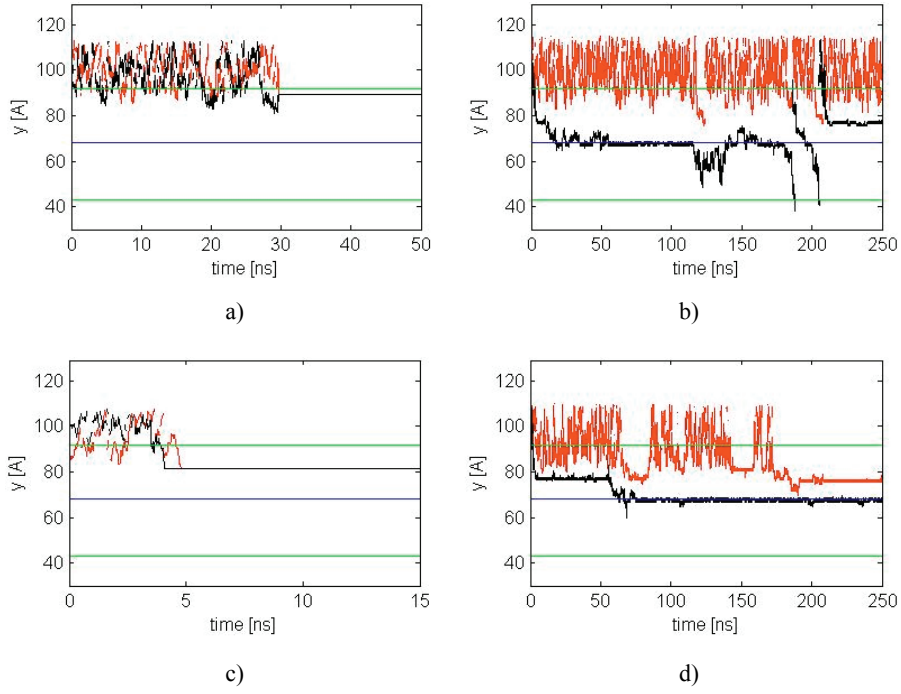

Fig. 5. The trajectories of the ions in 3fb8 simulations with: (a) irregular-sphere, (b) irregular-point, (c) circular-sphere, (d) circular-point, where red are the chloride anions, black are the potassium cations, green are the edges of the protein, blue is the middle of the membrane

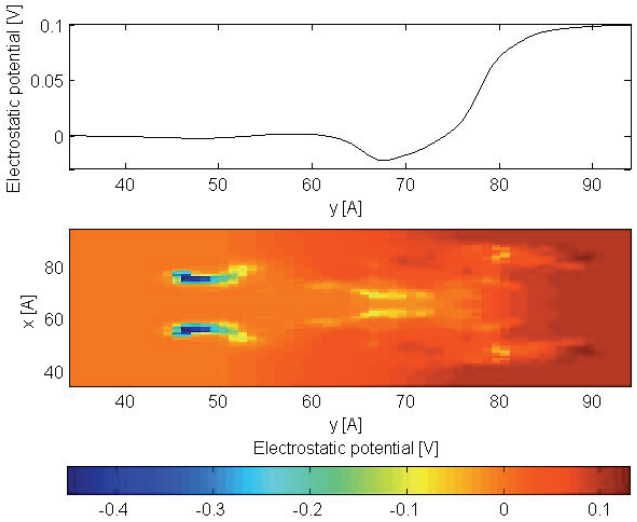

Fig. 6.The distribution of the electrostatic potential in 3fb8 simulation (down) and the electrostatic potential profile along the channel axis (up)

In simulations with the ion as a voxel we observed that the potassium ions went through the selectivity filter (from y = 66 Å to y = 81 Å). In the simulation with *irregular-point* (Fig. 5 b) two potassium ions passed through the whole channel. The second ion needed only 20 ns, while the first one was in the pore for 190 ns. The long period when the potassium ion resided in the filter was a result of the minimum electrostatic potential there (Fig. 6). If the positively charged ion wants to leave the filter it must overcome the 20 mV potential barrier. In natural conditions the interactions between the ions in the channel force the ion to leave the filter. However, only two ions with opposite charges were involved in our simulations, so only the random forces could help the ion to move on.

4. Discussion

IMBD provides BD simulations of nanopores, including narrow pores like the potassium channel KcsA, which is a problem for the publicly-accessible GCMC/BD program [19]. Our application allows us to observe the ions during the transition process, which can help to determine the properties of the channels. Moreover, publicly-accessible BD programs, mentioned earlier, are developed for UNIX platforms and, apart from GCMC/BD (the first three out of the five steps), they do not have any graphical interface. The IMBD program has been developed with Matlab so it can be used on either Windows or UNIX platforms. We are currently in the process of developing a graphical interface, which can be used optionally.

IMBD enables the selectivity of the charged ions, because in the simulations of the potassium channel only potassium ions passed through the pore as opposed to the alpha-hemolysin simulations, where the chloride anions were preferred according to the mildly anion-selectivity properties.

In our simulations the values of the forces which acted on the ions were in the proper ranges. But we can identify the problem of the not balancing the electrostatic Coulomb forces which cause the strong attraction between two oppositely charged ions. As our aim is to use BD simulations as a quality assessment of the protein structures, we need a fast tool, so we cannot calculate the non-electrostatic ion-ion potentials like Lennard–Jones potential in each step. Our idea is to prepare pre-calculated grids with the approximate potential values.

In this study we presented four versions of IMBD which differ from each other in terms of the ion definition or pore accessibility calculation. We have tested all combinations of the algorithm with two proteins: alpha-hemolysin and potassium channel KcsA.

Our results show that for wide pores, such as alpha-hemolysin, we should use van der Waals radii to describe the ion size (*sphere*). Within a narrow pore (potassium channel KcsA) simulation using the *sphere* representation the ions were blocked before the entrance to the selectivity filter. When the ion size is similar to the minimum pore diameter, the ion can be blocked in the pore. This problem results from the system representation with cubic voxels and a static protein during whole simulation. We can solve this problem with narrow pores by using the *point* representation of the ion. We would like to highlight that in the *point* method the ion's van der Waals radius is included in the value of the diffusion coefficient. Comparing the pore accessibility calculation methods, we noticed that in the *irregular* method there is a larger area available for ions in the pore, which could make ion transport faster or slower, depending on the pore width. In the case of the narrow pore the ions pass through the channel more easily, because the narrow path is made wider. On the other hand, for the wide pore the *irregular* method causes the formation of geometrical traps for ions and it can slow ion transport down. Hence, it seems that for narrow channels the *irregular* method would be more suitable, while for wide channels the *circular* method would be better.

In its current version, IMBD uses the electrostatic potential distribution from the 3D PNP Solver [15],

which includes the transmembrane potential and the ions in the pore. Moreover the 3D PNP Solver returns the potential from the last step of the ion flow iteration which corresponds to the equilibrium. We have also tested the influence of the potential grid sources on ion mobility. We noticed that the electrostatic potential distribution generated with the APBS [27] is not compatible with our BD algorithm. This is because the potential in the pore is too high in comparison to the external potential, which would constrain the ions' movement in one direction. The use of the APBS dictates that the charge should be smoothed. In papers by Aksimentiev [32], Cozmuta [14] and Dyrka [15] the charge was smoothed by applying a Gaussian distribution. This procedure allows us to obtain the representation which most closely resembles the physical channel profile.

In our next steps we will focus on improvement of the efficiency of the algorithm to shorten the CPU-time and reduce memory usage, by adding the pre-calculated Lennard-Jones potential grids, and we are preparing a similar procedure for Coulomb interactions.

Acknowledgements

Scientific work partially financed from the budget for science in 2012–2015 as a research project within the program "Diamond Grant" DI2011 002141. Some of the calculations have been performed in Wroclaw Centre for Networking and Supercomputing.

References

[1] KOZMA D., SIMON I., TUSNÁDY G.E., *PDBTM: Protein Data Bank of transmembrane proteins after 8 years*, Nucleic Acids Res., 2013,Vol. 41(Database issue), D275–D278.

[2] BERMAN H.M., WESTBROOK J., FENG Z., GILLILAND G., BHAT T.N., WEISSIG H., SHINDYALOV I.N., BOURNE P.E., *The Protein Data Bank*, Nucleic Acids Res., 2000, 28(1), 235–242.

[3] KROGH A., LARSSON B., VON HEIJNE G., SONNHAMMER E.L., *Predicting transmembrane protein topology with a hidden Markov model: application to complete genomes*, J. Mol. Biol., 2001, 305(3), 567–580.

[4] BARTH P., WALLNER B., BAKER D., *Prediction of membrane protein structures with complex topologies using limited constraints*, Proc. Natl. Acad. Sci. U.S.A., 2009, 106(5), 1409–1414.

[5] YU B., ZHANG Y., *A simple method for predicting transmembrane proteins based on wavelet transform*, Int. J. Biol. Sci., 2013, 9(1), 22–33.

[6] ASHCROFT F.M., *From molecule to malady*, Nature, 2006, 440(7083), 440–447.

[7] JAFRI M.S., KOTULSKA M., *Modeling the mechanism of metabolic oscillations in ischemic cardiac myocytes*, J. Theor. Biol., 2006, 242(4), 801–817.

[8] KOTA P., DING F., RAMACHANDRAN S., DOKHOLYAN N.V., *Gaia: automated quality assessment of protein structure models*, Bioinformatics, 2011, 27(16), 2209–2215.

[9] RATH E.M., TESSIER D., CAMPBELL A.A., LEE H.C., WERNER T., SALAM N.K., LEE L.K., CHURCH W.B., *A benchmark server using high resolution protein structure data, and benchmark results for membrane helix predictions*, BMC Bioinformatics, 2013, 14, 111.

[10] KONOPKA B.M., NEBEL J.C., KOTULSKA M., *Quality assessment of protein model-structures based on structural and functional similarities*, BMC Bioinformatics, 2012, 13, 242.

[11] DYRKA W., BARTUZEL M.M., KOTULSKA M., *Optimization of 3D Poisson-Nernst-Planck model for fast evaluation of diverse protein channels*, Proteins, 2013, 81(10), 1802–1822.

[12] KUYUCAK S., ANDERSEN O.S., CHUNG S-H., *Models of permeation in ion channels*, Rep. Prog. Phys., 2001, 64(11), 1427−1472.

[13] NOSKOV S.Y., IM W., ROUX B., *Ion permeation through the alpha-hemolysin channel: theoretical studies based on Brownian dynamics and Poisson-Nernst-Plank electrodiffusion theory*, Biophys. J., 2004, 87(4), 2299–2309.

[14] COZMUTA I., O'KEEFFE J.T., BOSE D., STOLC V., *Hybrid MD-Nernst Planck model of α-hemolysin conductance properties*, Mol, Simul,, 2005, 31, 79–93.

[15] DYRKA W., AUGOUSTI A.T., KOTULSKA M., *Ion Flux Through Membrane Channels – An Enhanced Algorithm for the Poisson-Nernst-Planck Model*, J. Comput. Chem., 2008, 29(12), 1876–1888.

[16] SCHIRMER T., PHALE P.S., *Brownian dynamics simulation of ion flow through porin*.

[17] CHUNG S.H., ALLEN T.W., KUYUCAK S., *Conducting-state properties of the KcsA potassium channel from molecular and Brownian dynamics simulations*, Biophys. J., 2002, 82(2), 628–645.

[18] KRISHNAMURTHY V., CHUNG S.H, *Adaptive Brownian dynamics simulation for estimating potential mean force in ion channel permeation*, IEEE Trans. Nanobioscience, 2006, 5(2), 126–38.

[19] LEE K.I., JO S., RUI H., EGWOLF B., ROUX B., PASTOR R.W., IM W., *Web interface for Brownian dynamics simulation of ion transport and its applications to beta-barrelpores*, J. Comput. Chem., 2012, 33(3), 331–339.

[20] KRAMMER E.M., HOMBLE F., PREVOST M., *Structure et Fonction des Membranes Biologiques*, Biochim. Biophys. Acta., 2013, 1828(4), 1284–1292.

[21] DE BIASE P.M., SOLANO C.J., MARKOSYAN S., CZAPLA L., NOSKOV S.Y., *BROMOC-D: Brownian Dynamics/Monte-Carlo Program Suite to Study Ion and DNA Permeation in Nanopores*, J. Chem. Theory Comput., 2012, 8(7), 2540–2551.

[22] GABDOULLINE R.R., WADE R.C., *Brownian Dynamics Simulation of Protein-Protein Encounter*, Methods, 1998, 3, 329–341.

[23] MADURA J.D., BRIGGS J.M., WADE R.C., DAVIS M.E., LUTY B.A., ILIN A., ANTOSIEWICZ J., GILSON M.K., BAGHERI B., SCOTT L.R, MCCAMMON J.A., *Electrostatic and diffusion of molecules in solution: simulations with the University of Houston Brownian Dynamics Program*, Comput. Phys. Commun., 1995, 91, 57–9.

[24] DŁUGOSZ M., ZIELIŃSKI P., TRYLSKA J., *Brownian dynamics simulations on CPU and GPU with BD_BOX*, J. Comput. Chem., 2011, 32, 2734–2744.

[25] CHUNG S.-H., KUYUCAK S., *Ion channels: recent progress and prospects*, Eur. Biophys. J., 2002, 31(4), 283−293.

[26] LOMIZE M.A., LOMIZE A.L., POGOZHEVA I.D., MOSBERG H.I., *OPM: Orientations of Proteins in Membranes database*, Bioinformatics, 2006, 22(5), 623−625.

[27] DOLINSKY T.J., CZODROWSKI P., LI H., NIELSEN J.E., JENSEN J.H., KLEBE G., BAKER N.A., *PDB2PQR: Expanding and upgrading automated preparation of biomolecular structures for molecular simulations*, Nucleic Acids Res., 2007, 35 (Web Server issue), W522−W525.

[28] BAKER N.A., SEPT D., JOSEPH S., HOLST M.J., MCCAMMON J.A., *Electrostatics of nanosystems: application to microtubules and the ribosome*, Proc. Natl. Acad. Sci. U.S.A., 2001, 98(18), 10037−10041.

[29] NOSKOV S.Y., WONPIL I., ROUX B., *Ion Permeation through the α-Hemolysin Channel: Theoretical Studies Based on Brownian Dynamics and Poissom-Nerst-Plank Electrodiffusion Theory*, Biophys. J., 2004, 87(4), 2299−2309.

[30] SONG L., HOBAUGH M.R., SHUSTAK C., CHELEY S., BAYLEY H., GOUAUX J.E., *Structure of staphylococcal alpha-hemolysin, a heptameric transmembrane pore*, Science, 1996, 274(5294), 1859−1866.

[31] DOYLE D.A., MORAIS-CABRAL J., PFUETZNER R.A., KUO A., GULBIS J.M., COHEN S.L., CHAIT B.T., MACKINNON R., *The structure of the potassium channel: molecular basis of K^+ conduction and selectivity*, Science, 1998, 280(5360), 69−77.

[32] AKSIMENTIEV A., SCHULTEN K., *Imaging alpha-hemolysin with molecular dynamics: Ionic conductance, osmotic permeability and the electrostatic potential map*, Biophys. J., 2005, 88, 3745–3761.